Operating synchrotron light sources with a high gain free electron laser

2015 New J. Phys. 17 113006

(http://iopscience.iop.org/1367-2630/17/11/113006)

New Journal of Physics
The open access journal at the forefront of physics

Deutsche Physikalische Gesellschaft DPG
IOP Institute of Physics

Published in partnership with: Deutsche Physikalische Gesellschaft and the Institute of Physics

OPEN ACCESS

RECEIVED
22 June 2015

REVISED
28 September 2015

ACCEPTED FOR PUBLICATION
2 October 2015

PUBLISHED
26 October 2015

PAPER

Operating synchrotron light sources with a high gain free electron laser

S Di Mitri[1] **and M Cornacchia**

Elettra-Sincrotrone Trieste S.C.p.A., Basovizza, I-34149, Italy
[1] Author to whom any correspondence should be addressed.

E-mail: simone.dimitri@elettra.eu

Keywords: high gain free electron laser, synchrotron light source, magnetic bunch length compression

Abstract

Since the 1980s synchrotron light sources have been considered as drivers of a high repetition rate (RR), high gain free electron laser (FEL) inserted in a by-pass line or in the ring itself. As of today, the high peak current required by the laser is not deemed to be compatible with the standard multi-bunch filling pattern of synchrotrons, and in particular with the operation of insertion device (ID) beamlines. We show that this problem can be overcome by virtue of magnetic bunch length compression in a ring section, and that, after lasing, the beam returns to equilibrium conditions without beam quality disruption. Bunch length compression brings a double advantage: the high peak current stimulates a high gain FEL emission, while the large energy spread makes the beam less sensitive to the FEL heating and to the microwave instability in the ring. The beam's large energy spread at the undulator is matched to the FEL energy bandwidth through a transverse gradient undulator. Feasibility of lasing at 25 nm is shown for the Elettra synchrotron light source at 1 GeV, and scaling to shorter wavelengths as a function of momentum compaction, beam energy and transverse emittance in higher energy, larger rings is discussed. For the Elettra case study, a low (100 Hz) and a high (463 kHz) FEL RR are considered, corresponding to an average FEL output power at the level of $\sim$1 W ($\sim 10^{13}$ photons per pulse) and $\sim$300 W ($\sim 10^{11}$ photons per pulse), respectively. We also find that, as a by-product of compression, the $\sim$5 W Renieri's limit on the average FEL power can be overcome. Our conclusion is that existing and planned synchrotron light sources may be made compatible with this new hybrid IDs-plus-FEL operational mode, with little impact on the standard beamlines functionality.

1. Background and outlook

Free electron lasers (FELs) in the ultra-violet (UV) and x-rays driven by high brightness radiofrequency linear accelerators (RF linacs) [1, 2] have become complementary to synchrotron light sources for the investigation of matter, from molecular to atomic scale. Despite their high peak brilliance and degree of coherence, high gain FELs are surpassed by synchrotrons in number of pulses per second and in number of beamlines that can be served simultaneously. A high repetition rate (RR) of the FEL is a prerequisite for multi-beamline operation; with present technology, it requires a superconducting linac [3–5] and a complex fan-like set of transfer lines [6].

Since the 1980s synchrotron light sources have been considered for driving a high gain self-amplified spontaneous emission (SASE) FEL [7, 8] in a by-pass line [9–16] or in the ring itself [17], in order to approach RRs of up to 100 kHz without a superconducting linac investment, and taking advantage of existing or planned synchrotron light sources. At present, synchrotron light sources target emittances compatible with lasing at (sub-)nm wavelength [18, 19], whereas FELs require emittances at the diffraction limit, $4\pi\varepsilon_x \leqslant \lambda$ [20]. Transverse gradient undulators (TGUs) [21, 22], traversed by an energy-dispersed beam, promise to compensate for the mismatch of large beam energy spread and FEL energy bandwidth [23, 24]. A single bunch peak current of up to $\sim$250 A [15, 16] could then generate significant FEL peak power in a practical undulator length. Unfortunately, the bunch peak current in a multi-bunch filling pattern is of the order of only a few tens of

Amperes, as determined by the beam's equilibrium distributions in the presence of synchrotron radiation, and limited by collective effects. As of today, the bunch peak current remains the main conceptual obstacle to the compatibility of a high gain FEL with synchrotrons' conventional spontaneous emission operation.

The simultaneous presence of long and short bunches was proposed in [25] through the adoption of a 2-frequency RF distribution for the BESSY-II synchrotron light source. Unlike in a more common 'low-alpha' mode of operation (this is an optics arrangement for setting a low momentum compaction, which typically allows the storage of few short bunches at equilibrium), the 2-frequency scheme allows the storage of a standard multi-bunch filling pattern. The single bunch peak current, however, is limited to 100 A level by single bunch and coupled bunch instabilities. High frequency superconducting RF cavities were proposed in [15] for increasing the single bunch peak current in the PEP-X ring above the 100 A level. High order modes (HOMs) in the cavities and microwave instability, however, would in that case limit the average current to 10 mA. Following the seminal study in [26], magnetic bunch length compression and de-compression in dedicated insertions across an undulator has been sketched for the PETRA-III ring [27]. While promising FEL production in the presence of a multi-bunch filling pattern, the conditions required for lasing in PETRA-III are, however, far from the operational ones: very high charge per bunch (20 nC instead of standard 0.8 nC) and only few RF buckets filled (40 consecutive buckets out of 960 available). Other crucial aspects have not yet been investigated in the PETRA-III study, gaps that we intend to cover in this paper: preservation of the electron beam quality in the presence of magnetic compression, single particle dynamics and collective effects of the stored beam; the effect of a high repetition FEL process, faster than damping time, on the electron beam distributions; feasibility of a long undulator line in an existing synchrotron lattice; compatibility of the FEL operation with that of insertion device (ID) beamlines. The paper is organized as follows.

In section 2, we introduce the concept of non-equilibrium magnetic bunch length compression, where 'non-equilibrium' refers to beam manipulation in a ring section before entering the internal by-pass, and return to equilibrium conditions immediately after lasing, *without beam quality disruption*. In this way, a high peak current, large energy spread beam can be provided at the undulator. This avoids any concern about microwave instability, otherwise excited by a stationary high peak current, low energy spread beam stored in the ring. We also discuss strategies for satisfying high gain FEL requirements on the electron bunch length as a function of the ring's momentum compaction, and on the transverse emittance as a function of the FEL wavelength.

In section 3, we show effective control of the electron beam brightness through particle tracking runs. Simulation results for one compression-FEL-decompression loop are presented. We show that beam preparation for lasing requires careful design of the linear and nonlinear optics, both in the ring and in the extraction/injection arcs. A suitable optics design is critical for linearizing the compression process, protecting the beam emittance from optical aberrations and coherent synchrotron radiation (CSR) effects, and yet allowing the bunch train to be stored and used for ID beamlines.

On the basis of the simulation results, an analytical evaluation of the FEL performance in a by-pass is provided in section 4. A low RR FEL performance is depicted first. The single electron bunch dynamics is considered for illustrative purposes, then extended to a multi-bunch filling patter, i.e. to an FEL pulse train. The multi-bunch filling pattern is permitted by a proper scheme for bunch train injection and extraction, respectively, into and from the by-pass. We then show that lasing can be made compatible with *standard* synchrotron light sources' multi-bunch operation. In this scenario, the FEL production time scale is set by the electron beam's longitudinal damping time.

In the majority of the studies on this topic, the RR of a ring-based FEL is limited to the inverse of the longitudinal damping time, primarily in order to thermalize the beam energy spread at the equilibrium level. This is overcome in theory in [17], where a new equilibrium for the bunch peak current, energy spread and FEL output is reached, still within the limitation of single bunch operation. A similar high RR FEL scenario is here analysed in section 5, but in addition the compatibility with a multi-bunch filling pattern is shown.

Following operational considerations for the implementation of the proposed scheme in section 6, we conclude in section 7 that a synchrotron in multi-bunch mode can simultaneously serve ID beamlines, and, by virtue of compression, at least one high gain FEL beamline fed by hundreds of Amperes peak current bunches. It is worth pointing out that bunch length compression brings a double advantage, as it provides high peak current and large energy spread at the undulator's entrance. The former stimulates a high gain FEL emission, the latter makes the beam less sensitive to the FEL-induced energy spread. As a by-product of the non-equilibrium compression, the Renieri's limit for the maximum average FEL power [28] is overcome, a limit that has been proved valid in low gain storage ring-based FELs. As a result, the proposed synchrotron light source may approach the performance of high average power FEL designs based on superconducting RF linac technology, and therefore satisfy many of the science cases related to those facilities [29–32], when a proper scaling of the proposed scheme to the wavelength of interest is considered. This study does not pretend to exhaust the comparison of ring-based high gain FELs w.r.t. linac-driven FELs. Still, it shows that existing and planned synchrotron light sources may be made compatible with this new hybrid ID-plus-FEL operational mode.

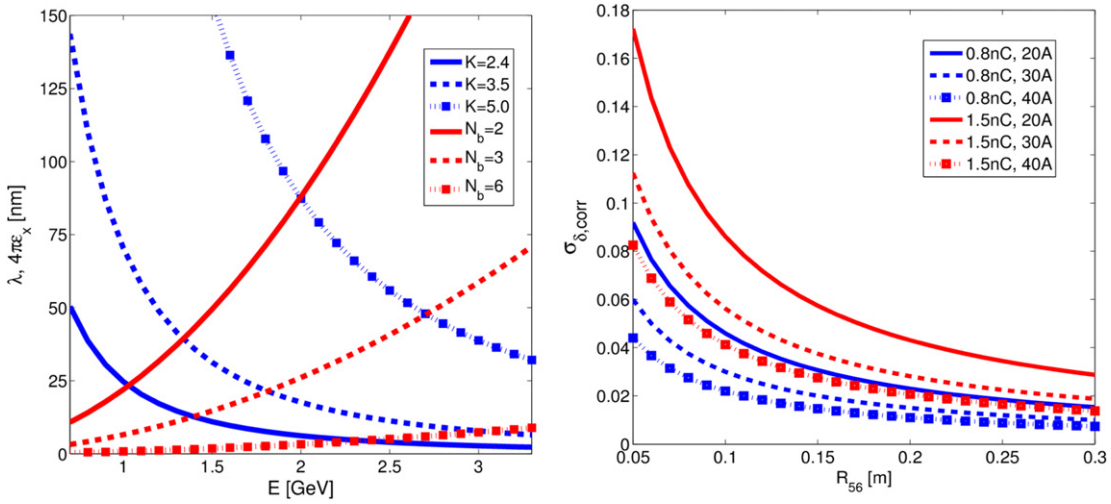

Figure 1. Left: Elettra equilibrium horizontal emittance for different number of dipoles per cell (red), and FEL wavelength for different undulator parameters (blue), versus beam energy (analytical). Right: rms relative correlated energy spread versus R_{56}, to reach 450 A starting from an initial peak current of 20–40 A, and for a bunch charge of 0.8 (blue) and 1.5 nC (red), see also equation (1). Energy and R_{56} span over ranges typical of mid size synchrotron light sources.

2. Bunch length compression and transverse emittance

The concept of beam manipulation is introduced first for a single bunch; the Elettra synchrotron [33] is used as a case study of lasing in the ultra-violet (UV). The 259 m long Elettra circumference may internally host a by-pass undulator line ∼60 m long at most, with ∼20 m left for beam extraction, optics matching to the undulator line and re-injection into the ring. With the one-dimensional (1D) TGU–SASE model introduced in [23, 24], we estimate a saturation length of around 50 m for an FEL radiating at 25 nm, and driven by ∼450 A peak current, ∼1% relative energy spread beam.

The FEL fundamental wavelength is shown in figure 1-left plot as a function of the beam energy, and defined by the resonance condition $\lambda = (\lambda_u/2\gamma^2)(1 + K^2/2)$, where γ is the relativistic Lorentz factor for the beam energy, λ_u is the undulator period length, $K = eB_0\lambda_u/(2\pi m_e c)$, typically in the range 1–5, is the so-called undulator parameter for a planar undulator, B_0 is the undulator peak magnetic field, e, m_e and c are the electron charge, rest mass and speed of light in vacuum, respectively. The Elettra horizontal equilibrium emittance is shown in the same plot as a function of beam energy ($\varepsilon_x \propto E^2$) and number of dipole magnets in an achromatic cell ($\varepsilon_x \propto 1/N_b^3$; $N_b = 2$ for the actual lattice). At $\lambda = 25$ nm, the diffraction limit $\varepsilon_x = \lambda/(4\pi) \approx 1.8$ nm is reached at $E = 1.0$ GeV (see intersection of solid blue and red curve in figure 1); we adopt that energy for the purpose of illustrating the principle of the lasing scheme. The FEL resonance condition is satisfied for $g/\lambda_u = 0.26$ ($g = 14$ mm is the undulator full gap), i.e., $K = 2.4$ [34].

We assume to install an S-band RF cavity in a straight section of the ring, and to run it at the phase of zero-crossing. A linear correlation in the electron longitudinal phase space (z, E) is established (henceforth called 'energy chirp'), and the bunch length is shortened by means of the momentum compaction α_c of the downstream ring section, in our example one half of the Elettra circumference. The following relationship has to be fulfilled by the energy chirp h, the RF peak voltage V, the bunch length compression factor C and $R_{56} = \alpha_c C_R/2$ of half the circumference length C_R:

$$h \equiv \left(\frac{1}{C} - 1\right)\frac{1}{R_{56}} = \frac{1}{E}\frac{\mathrm{d}E}{\mathrm{d}z} = \frac{2\pi}{\lambda_{\mathrm{RF}}}\frac{eV\cos\varphi_{\mathrm{RF}}}{E_0 + eV\sin\varphi_{\mathrm{RF}}} \approx \frac{\sqrt{\sigma^2_{\delta\mathrm{cor},0} + \sigma^2_{\delta\mathrm{unc},0}}}{\sigma_{z,0}}. \quad (1)$$

In equation (1), λ_{RF} is the RF wavelength, φ_{RF} (=0) the RF phase (at zero-crossing), $\sigma_{\delta\mathrm{cor},0}$, $\sigma_{\delta\mathrm{unc},0}$, and $\sigma_{z,0}$, the energy spread correlated with z, the uncorrelated energy spread and the bunch length *before* compression, respectively. In our example, $R_{56} = 0.21$ m, $\sigma_{\delta\mathrm{unc},0} = 0.1\%$ and $\sigma_{z,0} = 2.7$ mm. The chirp that provides minimum bunch length, i.e., maximum peak current at the end of compression is $h = -1/R_{56} = -4.8$ m^{-1}. The shortest bunch length we can achieve is $R_{56}\sigma_{\delta\mathrm{unc},0} = 210$ μm, and therefore the maximum effective compression factor is $C = \sigma_{z,0}/(R_{56}\sigma_{\delta\mathrm{unc},0}) \approx 13$. With a bunch charge $Q = 0.8$ nC, a peak current $I = CQc/(\sqrt{2\pi}\,\sigma_{z,0}) = 450$ A is provided at the undulator. Linear compression is guaranteed as long as the correlated energy spread is larger than the uncorrelated one; the latter evolves during compression according to $\sigma_{\delta\mathrm{unc}} = C\sigma_{\delta\mathrm{unc}0}$, because of longitudinal emittance preservation (i.e., the bunch length is shortened by a

Table 1. Major Elettra and electron parameters, used for particle tracking in section 3. 'Initial' values for the electron beam parameters refer to the equilibrium condition, i.e. before bunch length compression.

Circumference length	259.2	m
Harmonic number	432	
Number of filled buckets	$\leqslant$410	
Max. average current	380	mA
Longitudinal damping time	10	ms
Beam mean energy	1.0	GeV
Bunch charge	0.8	nC
Initial bunch duration, rms	9	ps
Initial peak current	35	A
Initial transverse emittance, rms	1.80(x), 0.02(y)	nm
Initial energy spread, rms	0.1	%
S-band RF peak voltage	78	MV
Energy chirp due to RF	-4.8	m^{-1}
R_{56} of half circumference	0.21	m
Compression factor	13	
Bunch duration at FEL, rms	0.7	ps
Peak current at FEL	455	A
Total energy spread at FEL	1.3	%
Transverse emittance at FEL, rms	2.15(x), 0.02(y)	nm
FEL fundamental wavelength	25	nm
Undulator parameter	2.5	
Undulator period	46	mm
Undulator length	55	m
TGU gradient	65.7	m^{-1}
Vertical dispersion at FEL	0.022	m
Average (β_x, β_y) along TGU	20(x), 10(y)	m
Average beam size along TGU, rms	0.20(x), 0.29(y)	mm

factor C, whereas the uncorrelated energy spread increases by the same factor). Hence, we require $\sigma_{\delta\mathrm{cor},0} \gg \sigma_{\delta\mathrm{unc}}$, where $\sigma_{\delta\mathrm{unc}} = \sigma_{\delta\mathrm{unc}0} = 0.1\%$ at equilibrium, and where $\sigma_{\delta\mathrm{unc}}$ approaches 1.3% when $C \rightarrow 13$. At the same time, $\sigma_{\delta\mathrm{cor},0}$ has to be not much larger than the synchrotron momentum acceptance, nominally 3% in Elettra, to avoid particle losses. With the parameters above, equation (1) specifies $V \approx 76$ MV and $\sigma_{\delta\mathrm{cor},0} \approx 1.3\%$, see also table 1.

Figure 1-right plot is the analytical representation of equation (1), and it suggests that, for any C and $\sigma_{z,0}$, a large R_{56} is desirable to minimize h, thus $\sigma_{\delta\mathrm{cor},0}$. A large R_{56}, however, is usually in conflict with the requirement of a low-emittance beam, which is the prerequisite for efficient lasing at short wavelengths. In fact, in modern synchrotron light sources with $E \geqslant 3.0$ GeV and $C_R \geqslant 500$ m [35, 36], ε_x is typically kept at the level of, or less than, few nanometers by multi-bend cells [37]. These cells imply α_c considerably smaller than in the Elettra double bend achromat (DBA)-based lattice, for which $\alpha_c = 1.6 \times 10^{-3}$, and R_{56} per turn smaller by a factor 2 to 5 than in Elettra. For this reason, in order to get, e.g., C $\geqslant$ 10, a relatively large energy spread ($\sigma_{\delta\mathrm{cor},0} > 2\%$) might be required in higher energy, larger rings. A peak current lower than $\sim$400 A might be viable as well, as a larger circumference can host a longer undulator to reach useful FEL powers. Alternatively, a high-α_c optics may be implemented, though, in principle, at the expense of ε_x. Finally, a larger R_{56} might be cumulated in one or even more turns. It emerges from this discussion that the capability of a lattice to provide a diffraction limited emittance at the FEL wavelength is in conflict with the capability of providing a large R_{56}, required in turn to achieve the desired compression factor for any allowed energy chirp. A compromise in the magnetic lattice design has therefore to be met, which takes simultaneously care of the beam transverse (emittance) and longitudinal dynamics (compression).

3. Simulation of beam dynamics

After compression is accomplished, the electron beam is directed to an internal by-pass. The 90 deg extraction arc we consider is a copy of the one introduced in [38], re-adjusted in space for our purposes and enriched by 8 sextupoles to make it achromatic and isochronous, so that bunch length is not affected further. Few matching quadrupoles and a small vertical dog-leg at the end of the extraction line prepares the bunch for lasing in the by-pass. A vertical energy dispersion is created by the dog-leg at the level of 2 cm, and it propagates through the vertical TGU in order to ensure lasing even by those electrons far from the resonant energy. The beam is then

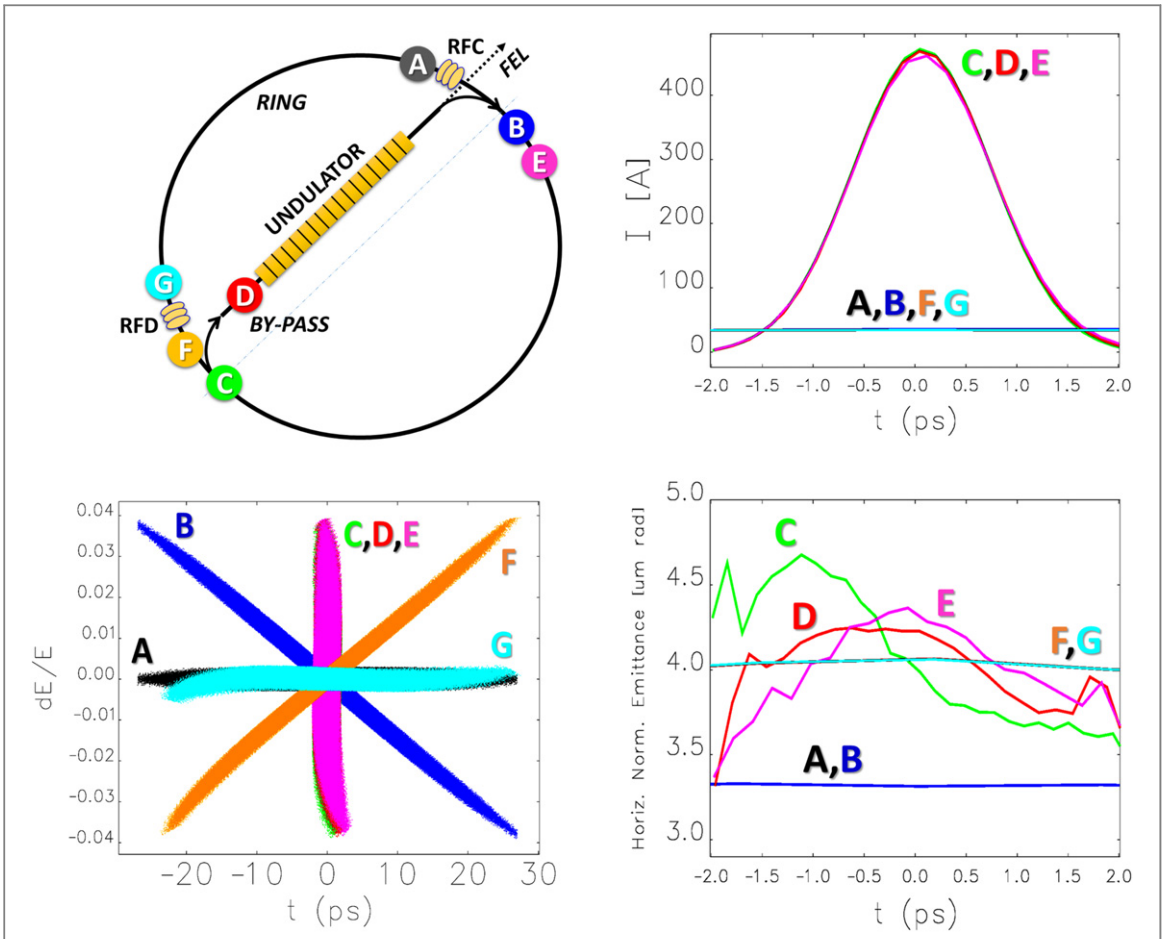

Figure 2. From top-left, clockwise: schematic of synchrotron ring with TGU in by-pass and RF cavities (RFC imposes the energy chirp, RFD removes it); single bunch peak current; slice horizontal emittance; longitudinal phase space, at the points marked with same labels and coloured circles in the schematic. A: equilibrium condition. B: energy chirp is added. C: compressed beam. D: entrance of undulator. E: exit of undulator (particle distribution at C, D, and E mostly overlaps in the longitudnal phase space and in the peak current plot). F: de-compressed beam. G: chirp is removed.

reinjected into the ring with a transfer line identical, but reversed, to that for extraction, which allows closure of the vertical dispersion. Since the compression has been tuned for an up-right longitudinal phase space at the undulator (minimum bunch length), the reinjected bunch will be decompressed in another half circumference, at the end of which an additional RF structure, identical to the first one, will remove the energy chirp. Such dynamics is illustrated in figure 2, where coloured circled labels in the layout correspond to the particle distributions in the other plots of the same figure (points A–G). It is worth mentioning that the interception of the FEL emission with the backward bend line of the ring (see figure 2-top left) is avoided by placing the undulator at a height above the synchrotron's plane: such a layout geometry is facilitated by the vertical dog-legs at the edges of the undulator, which are used to create vertical dispersion in the TGU.

Bunch length compression, transport to undulator and de-compression was simulated by tracking 5 million particles with the Elegant code [39], including up to 3rd order transport matrices, incoherent and coherent synchrotron radiation [40], with the initial beam parameters of table 1 (point A in figure 2). The strengths of 48 sextupoles in the ring were numerically optimized in order to simultaneously ensure: positive linear chromaticities, horizontal dynamic aperture larger than 10 mm at the injection point, ∼3% momemtum acceptance, and linear bunch length compression. Simulation studies indicate that simultaneous control of non-equilibrium emittance, linear chromaticity and nonlinear beam dynamics is facilitated by introducing more sextupoles per cell, and/or distributing them in more families, even independently supplied. Tracking results in figure 2, also summarized in table 1, confirm a beam quality at the undulator (point D) suitable for lasing in the UV wavelength range.

An important achievement of this study is the preservation of beam quality during (de-)compression and transport to/from the undulator. In particular, ε_x turns out to be substantially immune to CSR chromatic kicks [41, 42], by virtue of small horizontal betatron function in dipole magnets, optics symmetry and, in the ring, nearly-π phase advance across the DBA (see figure 3-left plot) [43–45]. In fact, low emittance optics in 3rd and 4th generation synchrotron light sources tend to minimize the so-called H-function averaged along the ring (see

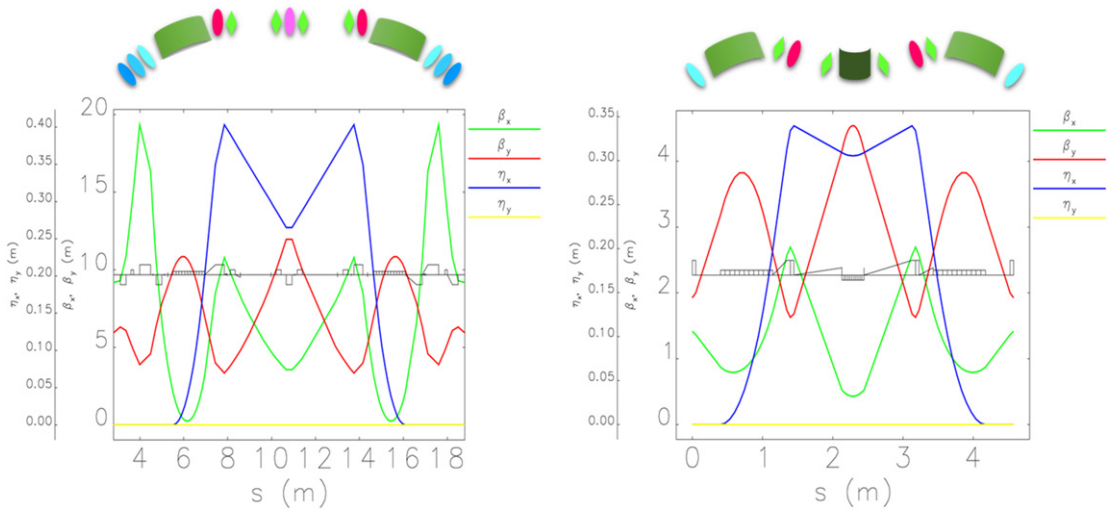

Figure 3. Linear optics functions for the Elettra DBA cell (left) and the cell of the extraction/reinjection arcs. A sketch of the magnetic lattice is shown on the top of each plot, with dipoles (rectangles), quadrupoles (ovals), and sextupoles (diamonds). The Elettra linear optics is the same as for normal ID beamlines operation; the nonlinear optics has been optimized in order to ensure both beam storage and linear compression. The arcs are achromatic and isochronous. Both in Elettra and in the arcs, the design optics allows the horizontal projected emittance to be largely immuned to CSR effect.

for example [46]). The latter, evaluated at the dipoles' location, is also responsible for the non-equilibrium CSR-induced emittance growth [44]. Thus, it is a remarkable property of low emittance lattices that of simultaneously minimizing the effect on emittance by incoherent and coherent photon emission. A CSR-immune optics design was also implemented in the extraction/re-injection arcs, and it is shown in figure 3-right plot.

4. Low RR FEL

4.1. Single bunch dynamics

If lasing is done at a RR smaller than the synchrotron longitudinal damping time, $\tau_s \approx 10$ ms in Elettra, a bunch is re-injected into the by-pass every time with parameters thermalized to equilibrium, i.e., each FEL pulse is generated like in a single pass device. The FEL-induced energy spread at saturation is expected to be not larger than $\sigma_{\delta,\mathrm{FEL}} = 1.6\rho_{\mathrm{TGU}} \approx 0.18\%$ [47], ρ_{TGU} being the TGU-modified FEL parameter [8, 24]. In the one-loop simulation depicted in figure 2, the effect of lasing was included by adding $\sigma_{\delta,\mathrm{FEL}}$ in quadrature to the energy spread of the compressed beam, $\sigma_{\delta\mathrm{unc}} \approx 1.3\%$ (point D); thus, the FEL modifies little the beam energy distribution. In fact, the FEL-spent electron beam is close to equilibrium, after de-compression and chirp removal, as shown by the particle distributions at point G in[2] figure 2. The electron beam vertical emittance is preserved at the 0.02 nm rad equilibrium level, in the assumption of 1% betatron coupling (see table 1).

The SASE saturation length and the peak power at saturation were evaluated as in the M.Xie 3D model [48], but now rescaled to the 1D TGU gain length, $L_{\mathrm{G,TGU}}$. This is sufficient for a preliminary optimization of beam sizes, undulator gradient and vertical dispersion (η_y) along the undulator. Figure 4 shows the analytical evaluation of the single pulse FEL output peak power at $\lambda = 25$ nm and after a 55 m long undulator, as a function of η_y, which regulates the FEL performance in the TGU [24], and of beam energy spread, which sets the compression factor (see equation (1)). $\sigma_{\delta\mathrm{cor},0} = 1.28\%$ allows one to achieve the maximum peak current of 455 A, and 138 MW FEL peak power when $\eta_y = 2.2$ cm. Average betatron functions $\beta_x = 20$ m, $\beta_y = 10$ m in the TGU ensure an almost round beam. With these parameters, $L_{\mathrm{G,TGU}} = 2.9$ m, and if we arbitrarily enlarge it by a factor 1.2 to take into account, for example, 3D effects [24], the peak power lowers to 47 MW. For the Reader's convenience, the main FEL parameters considered in this scenario are summarized in table 2, on the basis of the electron beam and the ring parameters listed already in table 1.

4.2. Multi-bunch filling pattern

The single bunch dynamics depicted so far applies equally well to a multi-bunch filling pattern, in which hundreds of bunches lie in RF buckets typically separated by 2 (Elettra) or few more nanoseconds. These can be

[2] We verified analytically through the 'sigma matrix formalism' that the one-pass contribution of the FEL-induced energy spread to the beam total energy spread and bunch length after re-injection into the ring, is negligible: the beam longitudinal emittance turns out to be preserved at the 0.1% level.

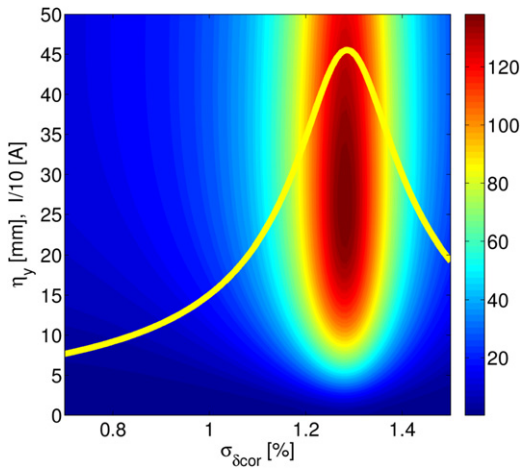

Figure 4. Contour plot of the estimated FEL peak power at saturation in MW versus rms relative energy spread and vertical dispersion in the TGU, for FEL repetition rate $\leqslant 1/\tau_s \approx 100$ Hz. Maximum power occurs for maximum peak current (yellow solid line), which is obtained for a correlated energy spread of 1.28%.

Table 2. Major FEL parameters at RR $\leqslant$ 100 Hz. Electron beam and storage ring parameters like in table 1.

FEL fundamental wavelength	25	nm
Undulator length	55	m
TGU-FEL parameter, 1D	0.11	%
FEL-induced energy spread, rms	0.18	%
TGU-gain length	2.9 (3.5)	m
FEL repetition rate	100	Hz
Number of bunches at FEL	360	
FEL pulse length, rms	0.7	ps
Number of photons, per pulse	1.6×10^{13} (0.5×10^{13})	
FEL peak power, per pulse	138 (47)	MW
FEL energy, per pulse	239 (81)	μJ
FEL average power, total	8.6 (2.9)	W

directed into/from the by-pass by kicker magnets or RF deflectors [49, 50]. Depending on the extraction scheme, different operational scenarios are possible.

For single bunch extraction with a kicker magnet, and a different bunch sent to FEL on consecutive extractions, the stored bunches have to be separated in time by twice the kicker's rise or fall time, τ_k. This allows the kicker to reach the required strength at the arrival time of the lasing bunch, without interfering with adjacent (earlier and later) bunches. An aggressive but still realistic $\tau_k \approx 4$ ns [50] permits to accommodate no more than 108 bunches in Elettra. We assume the kicker magnet working at 100 kHZ RR, so that the FEL output time structure will be made of macropulses emitted every $\tau_s \approx 10$ ms, each comprising up to 108 pulses separated by 10 μs from each other, as shown in figure 5-left plot. The total average FEL power turns out to be 2.6 W (0.9 W for the degraded $L_{G,TGU}$ considered above, see also table 2), at the RR of 100 Hz. In this scenario, the average stored current is limited to 100 mA, of the maximum available 380 mA, because the number of bunches is upper-limited by the kicker's rise and fall time.

The FEL time structure internal to the macropulse can be made more dense if bunch-by-bunch extraction/injection is done with an RF deflector. Owing to the intrinsic CW nature of the transverse electric field in such a cavity, an entire bunch train can be sent to/extracted from the by-pass. In this case, the maximum FEL RR is for a bunch train filling the B-C-D-B loop in figure 2, whose path length is equal to $(C_R/2 + L) \approx (5C_R/6)$. For a 2 ns bunch-to-bunch separation, the train contains 360 bunches at most, and the average current turns out to be 330 mA. Still, the train is lasing every 10 ms. The FEL average power is approximately 8.6 (2.9) W. This option is summarized in table 2 and depicted in figure 5-middle plot.

Alternatively, always the same bunch can be selected for lasing; this is shown in figure 5-right plot. Because of its path in the by-pass, the bunch will be shifted w.r.t. to its initial bucket position by approximately $(C_R/2 - L) \approx C_R/6$, with L the by-pass path length. We therefore have to reserve 6 gaps in the filling pattern, each gap distant τ_k in time from adjacent buckets, in which the bunch will jump at successive FEL loops, until it

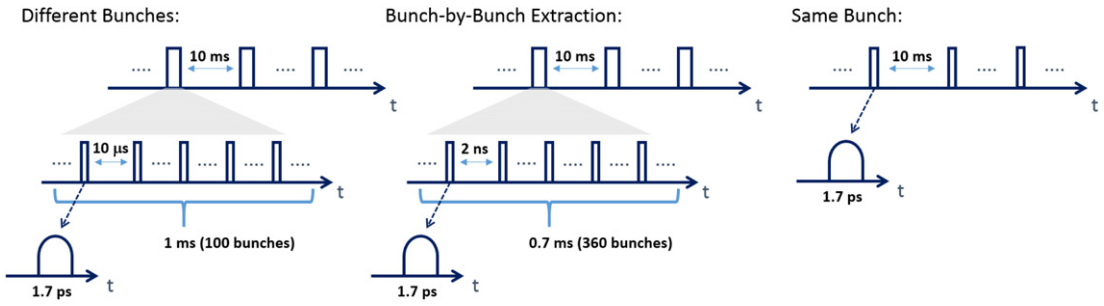

Figure 5. Schematic of FEL pulse time structure (see text above for details). In all the configurations, 10 ms macropulses separation corresponds to approximately one damping time in Elettra; the single FEL pulse is about 1.7 ps long (such a duration is only indicative and it reflects the FWHM electron bunch duration at full compression, see figure 2). Left: individual FEL pulses are separated by 10 μs, as dictated by the 100 kHz RR of the kicker magnet used for injection into the by-pass. Up to about 100 bunches and 100 mA average current can be hosted in this scheme. Middle: FEL pulses are separated by 2 ns, according to the Elettra harmonic number; 360 bunches and approximately 330 mA can be stored in this scheme. Right: same-bunch lasing every damping time; almost the maximum number of bunches and the nominal average current of 380 mA can be accumulated.

returns to its original bucket. This way, up to 408 bunches grouped in 6 trains, which will not be lasing, can be stored (almost the maximum number of bunches allowed by the operational filling pattern in Elettra, see table 1); they are interleaved by $2\tau_k \approx 8$ ns long gaps, where the lasing bunch is accommodated. The average stored current is 378 mA. Since the bunch will be lasing at least every damping time, in order to recover its equilibrium properties after FEL emission, the average FEL output power is now only 0.02 W at 100 Hz RR; the FEL time structure will resemble a CW mode, as shown in figure 5-right plot. Additional scenarios could be envisaged in the presence of multi-bunch extraction by hundreds of ns long kicker pulses [51, 52], although stability issues of the kicker pulse should then be properly evaluated.

5. High RR FEL

5.1. New equilibrium conditions

We can imagine operating kicker magnets or RF deflectors for a high RR laser production. As an example, we consider the adoption of RF deflectors that enable buncy-by-bunch manipulation. This time, unlike the scenario depicted in section 4, the bunch train will be lasing every 2 turns: after FEL production (point E in figure 2), half turn is devoted to de-compression, one turn and half for providing light to ID beamlines and for returning to the 'RF chirper' (point A). After 2 turns, the FEL cycle starts again.

Lasing at RRs higher than $1/\tau_s$ implies *new equilibrium conditions* for the stored beam. These are determined by the simultaneous action of the FEL, which enlarges the beam energy spread at every pass, and the longitudinal (i.e., energy) damping. We used the algorithm adopted in [17] (see also [53]) to evaluate beam current, energy spread and FEL peak power at the new equilibrium, with two important differences: the TGU-modified SASE model is adopted here for the FEL output, and the FEL-induced energy spread is reduced by a factor C due to bunch lengthening after lasing. The modified equation for the *uncompressed* beam's energy spread at the new equilibrium, $\sigma_{\delta,\mathrm{eq}}$, reads:

$$\frac{\mathrm{d}\sigma^2_{\delta,\mathrm{eq}}}{\mathrm{d}t} = \frac{\sigma^2_{\delta\mathrm{unc},0} - \sigma^2_{\delta,\mathrm{eq}}}{\tau_s} + \frac{1}{T_{\mathrm{FEL}}}\left(\frac{\sigma_{\delta,\mathrm{FEL}}}{C}\right)^2 \equiv 0. \tag{2}$$

Here T_{FEL} is the period of lasing (2 turns in our case), $\sigma^2_{\delta,\mathrm{FEL}} \approx 2\rho_{\mathrm{TGU}} P_{\mathrm{FEL}}/(eIE)$, $P_{\mathrm{FEL}} \approx 0.1 P_n \exp(z/L_{\mathrm{G,TGU}})$, and P_n the shot noise power of the electron beam at the undulator's entrance [17]. ρ_{TGU} and $L_{\mathrm{G,TGU}}$ depend in turn on the beam energy spread at the undulator [24]:

$$\rho_{\mathrm{TGU}} = \rho\left(1 + \frac{\eta_y^2 C^2 \sigma^2_{\delta,\mathrm{eq}}}{\sigma_y^2}\right)^{-1/6}. \tag{3}$$

ρ is the 1D FEL parameter [8] and σ_y the average electron beam size along the vertical TGU. Since $\rho \propto I^{1/3}$, with I the peak current *at the undulator*, equations (2) and (3) also take into account the dependence of I on the energy spread, namely $I = CI_{\mathrm{eq}} \propto C\sigma^{-1}_{\delta,\mathrm{eq}}$, as also assumed in [17]. It is important to notice that bunch length compression mitigates the FEL perturbation to the beam energy spread at each pass, as the sum of the two, after *one* compression and de-compression loop, is of the order of $\sqrt{(C\sigma_{\delta\mathrm{unc},0})^2 + \sigma^2_{\delta,\mathrm{FEL}}}/C$, where $C \gg 1$ and $\sigma_{\delta\mathrm{unc},0}$ is of the order of $\sigma_{\delta,\mathrm{FEL}}$. This dynamics is highlighted by the factor $(1/C)^2$ in equation (2). We also draw the Reader's attention to the fact that this large reduction of the FEL perturbation is a novel and much improved

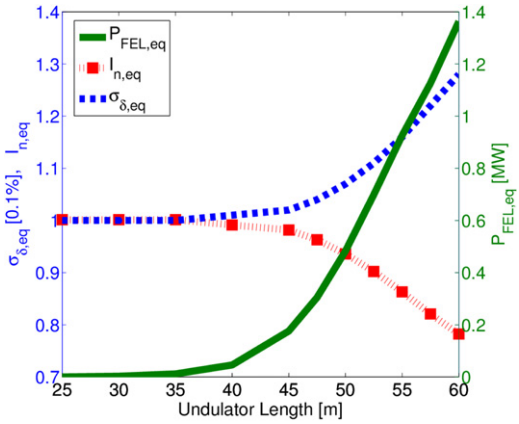

Figure 6. Rms relative energy spread of the uncompressed beam (blue dashed), peak current at FEL normalized to 450 A (red, dotted), and single pulse FEL output peak power (green, solid line), as a function of the undulator length; all parameters are at the *new equilibrium* established according to equation (2), when the FEL RR $>$ 100 Hz.

Table 3. Major electron beam and FEL parameters at RR $>$ 100 Hz (new equilibrium conditions, see text above). All other electron beam and storage ring parameters like in table 1.

FEL fundamental wavelength	25	nm
Undulator length	55	m
Peak current at FEL	380	A
Energy spread at equilibrium, rms	0.12	%
FEL repetition rate	463	kHz
Number of bunches at FEL	360	
FEL pulse length, rms	$\leqslant$0.7	ps
Number of photons, per pulse	1.1×10^{11}	
FEL peak power, per pulse	1.0	MW
FEL energy, per pulse	1.7	μJ
FEL average power, total	288	W

approach, not having been considered in previous ring-based FELs, in which the FEL induced energy spread adds to the beam energy spread as $\sqrt{\sigma_{\delta\mathrm{unc},0}^2 + \sigma_{\delta,\mathrm{FEL}}^2}$ [9–17].

The numerical evaluation of $\sigma_{\delta,\mathrm{eq}}$ in equation (2) as a function of the undulator length z is shown in figure 6, together with the peak current at the undulator and the single pulse FEL peak power. The choice of the undulator length can be used to balance FEL power and beam energy spread, in order to tune the operational parameters of the FEL versus those for the ID beamlines. One should notice that the FEL may also act as a damping wiggler for the transverse emittance at equilibrium. Although generally welcome, this additional effect should be balanced versus a potential enhancement of intra-beam scattering.

5.2. Operational considerations

Managing the energy chirp before and after compression at RRs $>$ 100 Hz requires high RF frequency normal conducting cavities, or even CW superconducting (SC) cavities, which have to sustain few hundreds of mA average current [54, 55]. As an example, and according to equation (1), the energy chirp listed in table 1 can be obtained with a SC 1.5 GHz multi-cells module, 8 m long and targeting 20 MV m^{-1}. As a result, and in the case of bunch-by-bunch extraction with an RF deflector, we are allowed to store 360 bunches for a total average current of 330 mA. According to figure 6, each bunch generates $\sim$1 MW FEL peak power at the end of a 55 m long undulator, at approximately 0.5 MHz RR, thus producing $\sim$288 W of total average FEL power. Table 3 summarizes the main electron beam and FEL output parameters at a RR $>$ 100 Hz, when the new equilibrium is established.

6. Discussion

We draw the Reader's attention to the fact that, unlike preceding works on this subject, we do not foresee any critical impact of microwave instability [56–61] on the beam dynamics, for the following reasons. First, in the low RR FEL scenario, the high single bunch peak current situation lasts for only one turn every damping time,

which is not long enough for the instability to build up. Second, the instability current threshold is proportional to the square of the beam energy spread [56], therefore it 'increases' by a factor $C^2 = 169$, when the beam is maximally bunched by a factor $C = 13$. In other words, at the point of maximum compression, i.e. maximum peak current, the instability is suppressed by the larger energy spread. In Elettra, the appearance of the instability has been recorded at $\geqslant$1 mA of average current per bunch at equilibrium, in the energy range 0.9–1.2 GeV [62]. Hence, when the peak current is increased by magnetic compression, we expect to be able to reach any practical average and peak current per bunch, without exciting the microwave instability.

It is important to point out that, depending on the filling pattern and the duration of the RF pulse in the (de-) chirper cavity, bunches not devoted to lasing may find RF power in the cavity at their passage through it, and thus be subjected to parasitic bunch length gymnastic. This might imply an effective reduction of the synchrotron duty cycle for those ID beamline experiments that are sensitive to either pulse duration (which depends on electron bunch length) or to bandwidth of the undulator spontaneous emission (possibly affected by a larger electron bunch's enery spread). In the bunch-by-bunch extraction (figure 5-middle plot), that parasitic gymnastic can be avoided, for example, by choosing a pulsed normal conducting cavity whose RF pulse duration is shorter than approximately one revolution period, e.g. ~800 ns. At the same time, the technical challenge of HOM dampers at room temperature should be considered.

A superconducting (SC) option for the cavity could alternatively be exploited, for which the HOM dampers technology is now well established. This option, however, implies RF fillling times typically not shorter than 1 ms, during which all bunches will 'rotate' in the longitudinal phase space. In the low RR FEL scenario, where the bunch train is stored in the ring for at least one damping time, i.e. 10 ms, before re-injection into the by-pass, the synchrotron duty cycle would be reduced (for specific experiments mentioned above) by approximately 1 ms/10 ms = 10%. In the high RR FEL case, with lasing every few turns, the full compatibility with ID beamlines operation might be solved *ab initio* by hosting the chirper and de-chirper RF cavities in short by-pass lines parallel to the ring straight sections: only those bunches devoted to lasing will be sent through the cavities by additional fast kicker magnets or RF deflectors. This solution obviously adds some complexity to the SC option.

Heating of the synchrotron's vacuum chamber by CSR emission, which is expected to be enhanced during bunch shortening, is another issue to be considered in a detailed technical design. The associated photodesorption, especially in the high RR FEL scenario, will probably imply a special design of cooling and vacuum system. On the contrary, the average power of the spontaneous radiation is of the same order as in conventional storage rings, and will not cause problems.

7. Conclusions

The present article introduces and demonstrates the in-principle feasibility of non-equilibrium short bunches in synchrotrons. We demonstrate that, by virtue of a reversible manipulation of the length of one or more bunches, existing and planned synchrotron light sources can be made compatible with a new high gain FEL + IDs operational mode, and that the scheme may even be applied to future storage ring-driven FELs. In the authors' opinion, the most relevant contribution of the present work is the realistic possibility of a storage ring lattice of compressing the bunch length without beam quality disruption, and its compatibility with a standard multi-bunch operation. The second relevant contribution is that the compression brings a double advantage: first, it provides a high peak current which is crucial for stimulating a high gain FEL emission; second, it enlarges the beam uncorrelated energy spread so that the beam is less sensitive both to the energy spread induced by the FEL itself, and to the microwave instability when a high peak current is produced. For the Elettra case study at 1 GeV, a low (100 Hz) and a high (463 kHz) FEL RR are considered, corresponding to an average FEL output power at the level of ~1 W (~10^{13} photons per pulse) and from ~10 to ~300 W (up to ~10^{11} photons per pulse), respectively, depending on the multi-bunch filling pattern and the scheme for injection into the FEL by-pass. The third relevant contribution is the demonstration that the Renieri's limit on the average FEL power, ~5 W in our case study, can be overcome when non-equilibrium bunch length compression is implemented [63]. The Renieri's limit is caused by the enlarged energy spread of the beam after lasing when the *same* beam parameters apply to both ring and FEL [64]. With non-equilibrium compression, instead, the electron beam reaches transient longitudinal distributions at the undulator, which are different from those of the stored, uncompressed beam.

Being a conceptual design study, the present work does not aim to analyse in detail all the technical aspects. Neverthelss, the main relevant issues have been given attention and, we believe, at least conceptually solved. Wakefield induced beam heating and quality degradation, vacuum chamber cooling and feedback systems are all issues that detailed designs will have to address. It is probable that special care in the design of the undulator and ring vacuum systems will have to be used to keep the wakefield impedence within an acceptable level.

In summary, unlike previous studies contemplating the use of a stored beam to generate a high gain FEL, our proposal allows the following improvements: simultaneous, multi-bunch FEL + IDs operation; FEL RR comparable to, and FEL peak power ring-based low gain single-pass FELs and FEL oscillators [65–72] at same wavelengths [74]. With respect to FEL oscillators, shorter wavelengths become accessible by virtue of a mirror-free optical architecture, although some recent progress might allow x-ray FEL oscillators to be feasible in the near future [73, 74]; negligible radiation issues w.r.t. energy-recovery linacs, at similar peak and average FEL performance. It is worth mentioning that exotic (hybrid) filling patterns and intermediate RRs could be considered in addition to those discussed so far, providing FEL and ID beamline performance somewhere in between the scenarios depicted above. Moreover, the proposed scheme does not prevent form considering FEL architectures other than SASE: OK-SASE [75] promises higher FEL power or a shorter undulator line; externally- or self-seeded FEL schemes [76–80] may provide sub-ps FEL pulse duration, shorter wavelengths and/or narrower spectral bandwdth.

Acknowledgment

The authors are in debt to F Parmigiani for a discussion on the impact of a by-pass FEL on synchrotrons performance, and with R Hettel for valuable suggestions regarding operational aspects of our proposal. The authors acknowledge Z Huang for comments about the compatibility of a by-pass FEL and multi-bunch filling patterns, B Diviacco for a discussion on the TGU concept, M Placidi for information on kicker magnets and RF deflectors, and D Garzella for a discussion on the Renieri's limit. This work was funded by the FERMI project, the ODAC project, and the Accelerators Group of Elettra Sincrotrone Trieste.

References

[1] Blau J, Cohn K, Colson W B and Tomlinson W 2014 *Proc. 36th Int. Free Electron Laser Conf.* TUP088 (*Basel, Switzerland*)
[2] Mitri S D and Cornacchia M 2014 *Phys. Rep.* **539** 1–48
[3] Feldhaus J 2010 *J. Phys.* B **43** 194002
[4] Altarelli M 2011 *Nucl. Instrum. Methods Phys Res.* B **269** 2845–9
[5] Galayda J N 2014 *Proc. Int. LINAC Conf.* TUIOA04 (*Geneva, Switzerland*)
[6] Honkavaara K, Faatz B, Feldhaus J, Schreiber S, Treusch R and Vogt M 2014 *Proc. 36th Int. Free Electron Laser Conf.* WEB05 (*Basel, Switzerland*)
[7] Kondratenko A M and Saldin E L 1980 *Part. Accel.* **10** 207–16
[8] Bonifacio R, Pellegrini C and Narducci L M 1984 *Opt. Commun.* **50** 373–8
[9] Murphy J B and Pellegrini C 1985 *Nucl. Instrum. Methods Phys. Res.* A **237** 159–67
[10] Kim K-J-, Bisognano J J, Garren A A, Halbach K and Peterson J M 1985 *Nucl. Instrum. Methods Phys. Res.* A **239** 54–61
[11] Kim K-J *et al* 1985 *IEEE Trans. Nucl. Sci.* **5** 3377–9 NS-32
[12] Bisognano J *et al* 1986 *Part. Accel.* **18** 223–66
[13] Cornacchia M *et al* 1986 *Nucl. Instrum. Methods Phys. Res.* A **250** 57–63
[14] Nuhn H-D, Fisher A S, Gallardo J C, Pellegrini C, Tatchyn R and Winick H 1992 *Nucl. Instrum. Methods Phys. Res.* A **319** 89–96
[15] Cai Y, Ding Y, Hettel R, Huang Z, Wang L and Xiao L 2013 *Synchrotron Radiat. News* **26** 39–41
[16] Ding Y, Baxevanis P, Cai Y, Huang Z and Ruth R 2013 *Proc. 4th Int. Particle Accel. Conf.* WEPWA075 (*Shanghai, China*)
[17] Huang Z, Bane K, Cai Y, Chao A, Hettel R and Pellegrini C 2008 *Nucl. Instrum. Methods Phys. Res.* A **593** 120
[18] Borland M *et al* 2014 *Synchrotron Radiat. News* **27** 2–31
[19] Cai Y, Bane K L, Hetel R, Nosochkov Y, Wang M H and Borland M 2012 *Phys. Rev. Spec. Top. Accel. Beams* **15** 054002
[20] Kim K-J 1986 *Nucl. Instrum. Methods Phys. Res.* A **246** 71–6
[21] Smith T, Madey J M J, Elias L R and Deacon D A G 1979 *J. Appl. Phys.* **50** 4580
[22] Kroll N, Morton P, Rosenbluth M, Eckstein J and Madey J M J 1981 *IEEE J. Quantum Electron.* **17** 1496
[23] Huang Z, Ding Y and Schroeder C B 2012 *Phys. Rev. Lett.* **109** 204801
[24] Baxevanis P, Ding Y, Huang Z and Ruth R 2014 *Phys. Rev. Spec. Top. Accel. Beams* **17** 020701
[25] Wüstefeld G *et al* 2011 *Proc. 1st Int. Part. Accel. Conf.* THPC014 (*San Sebastián, Spain*) p 2936
[26] Hofmann A 1986 SSRL ACD-Note 39 unpublished
[27] Agapov I 2015 *Nucl. Instr. Meth. Phys. Research* A **793** 35–40
[28] Renieri A 1979 *IEEE Trans. Nucl. Sci.* NS- **26** 3827
[29] Marangos J *et al* 2010 *New Light Source Conceptual Design Report* pp 17–92 (http://newlightsource.org/documents/NLS%20CDR%20Consolidated%20Final.pdf)
[30] Corlett J *et al* 2010 *Next Generation Light Source CD-0 Proposal* pp 5–105 (http://2.lbl.gov/ngls/science/)
[31] Arthur J *et al* 2013 *Science Driven Instrumentation for LCLS-II* pp 5–51 (https://portal.slac.stanford.edu/sites/-lcls_public/Instrument_Document_Repository/LCLS-II_Instrumentation_Whitepaper_DOE.pdf)
[32] Schneidmiller E, Vogel V F, Weise H and Yurkov M V 2012 *J. Micro/Nanolith. MEMS MOEMS* **11** 021122
[33] Karantzoulis E, Carniel A and Krecic S 2014 *Proc. 5th Int. Particle Accel. Conf.* MOPRO076 (*Dresden, Germany*)
[34] Clarke J A 2004 The science and technology of undulators and wigglers (*Oxford Series on Synchrotron Radiation* vol 4) (Oxford: Oxford University Press) p 118
[35] Bei M *et al* 2010 *Nucl. Instrum. Methods Phys. Res.* A **622** 518–35
[36] Hettel R 2014 *Proc. 5th Int. Part. Accel. Conf.* MOXBA01 (*Dresden, Germany*)
[37] Leemann S C, Andersson Å, Eriksson M, Lindgren L-J, Wallén E, Bengtsson J and Streun A 2009 *Phys. Rev. Special Topics—Accel. Beams* **12** 120701
[38] Douglas D *et al* 2014 JLAB-ACP-14-1751 arXiv:1403.2318

[39] Borland M 2000 A P S Tech Note LS-207
[40] Borland M 2001 *Phys. Rev. Spec. Top.—Accel. Beams* **4** 070701
[41] Nakazato T *et al* 1989 *Phys. Rev. Lett.* **63** 2433
[42] Derbenev Y S, Rossbach J, Saldin E L and Shiltsev V D 1995 *TESLA-FEL* 95–05, DESY (*Hamburg, Germany*)
[43] Douglas D 1998 JLAB-TN-98-012
[44] Mitri S D, Cornacchia M and Spampinati S 2013 *Phys. Rev. Lett.* **110** 014801
[45] Mitri S D and Cornacchia M 2015 *Europhys. Lett.* **109** 62002
[46] Leemann S C and Streun A 2011 *Phys. Rev. Spec. Top.—Accel. Beams* **14** 030701
[47] Saldin E L, Schenidmiler E A and Yurkov M V 2000 *The Physics of Free Electron Lasers* (Berlin: Springer) p 62
[48] Xie M 1995 *Proc. 16th Part. Accel. Conf.* TPG10 (*Dallas, USA*)
[49] Naito T, Hayano H, Kuriki M, Terunuma N and Urakawa J 2007 *Nucl. Instrum. Meth. Phys. Res.* A **571** 599
[50] Placidi M, Jung J-Y, Ratti A and Sun C 2014 *Nucl. Instrum. Meth. Phys. Res.* A **768** 14–9
[51] Niell F *et al* 2014 *Proc. 30th Int. Part. Accel. Conf.* MOPME081 (*Dresden, Germany*)
[52] Holma J, Barnes M J and Belver-Aguilar C 2014 *Proc. 30th Intern. Part. Accel. Conf. MOPRO028* (*Dresden, Germany*)
[53] Ellaume P 1984 *J. Phys.* **45** 997–1001
[54] Benson S V *et al* 2011 *J. Mod. Opt.* **58** 1438–51
[55] Liu Z and Nassiri A 2010 *Phys. Rev. Spec. Top.—Accel. Beams* **13** 012001
[56] Hofmann A 1977 *CERN 77-13* ed M H Blewett (Geneva: CERN) p 139
See also Stupakov G and Heifets S 2002 *Phys. Rev. Spec. Top.—Accel. Beams* **5** 054402
[57] Krinsky S and Wang J M *Part. Accel.* 1985 **17** 109
[58] Bosser J *et al* 2000 *Nucl. Instrum. Methods Phys. Res.* A **441** 1
[59] Warnock R 2005 *Phys. Rev. Spec. Top.—Accel. Beams* **8** 014402
[60] Cai Y 2011 *Phys. Rev. Spec. Top.—Accel. Beams* **14** 061002
[61] Roussel E *et al* 2014 *Phys. Rev. Lett.* **113** 094801
[62] Karantzoulis E, Penco G, Perucchi A and Lupi S 2010 *Infrared Phys. Technol.* **53** 300–3
[63] Another example of Renieri's limit break is illustrated in Litvinienko V N 1996 *Nucl. Instrum. Methods Phys. Res.* A **375** 584–8
[64] Dattoli G *et al* 2012 *IEEE J. Quantum Electr.* **48** 10
[65] Girard B *et al* 1984 *Phys. Rev. Lett.* **53** 2405
[66] Doyuran A *et al* 2001 *Phys. Rev. Lett.* **86** 5902
[67] Litvinenko V *et al* 2001 *Nucl. Instrum. Methods Phys. Res.* A **475** 195
[68] Trovò M *et al* 2002 *Nucl. Instrum. Methods Phys. Res.* A **483** 157
[69] Yu L H *et al* 2003 *Phys. Rev. Lett.* **91** 074801
[70] Labat M *et al* 2007 *Eur. Phys. J. D* **44** 187
[71] De Ninno G *et al* 2008 *Phys. Rev. Lett.* **100** 104801
[72] De Ninno G *et al* 2008 *Phys. Rev. Lett.* **101** 053902
[73] Kim K-J *et al* 2008 *Phys. Rev. Lett.* **100** 244802
[74] Lindberg R R, Kim K-J, Cai Y, Ding Y and Huang Z 2013 *Proc. 35th Int. Free Electron Laser Conf.* THOBNO02 (*New York, USA*)
[75] Penco G, Allaria E, De Ninno G, Ferrari E and Giannessi L 2015 *Phys. Rev. Lett.* **114** 013901
[76] Allaria E *et al* 2012 *Nat. Photonics* **6** 699–704
[77] Allaria E *et al* 2013 *Nat. Photonics* **7** 913–8
[78] Xiang D *et al* 2010 *Phys. Rev. Lett.* **105** 114801
[79] Feng C, Deng H, Wang D and Zhao Z 2014 *New J. Phys.* **16** 043021
[80] Ratner D *et al* 2015 *Phys. Rev. Lett.* **114** 054801